



ELSEVIER

Journal of Membrane Science 99 (1995) 217–228

Journal of  
MEMBRANE  
SCIENCE

## Characterization of hemodialysis membranes by inverse size exclusion chromatography

Arnold P. Broek<sup>1,a</sup>, Herman A. Teunis<sup>a</sup>, Derk Bargeman<sup>a</sup>, Erik D. Sprengers<sup>b</sup>,  
Heiner Strathmann<sup>a,\*</sup>, Cees A. Smolders<sup>a</sup>

<sup>a</sup> University of Twente, Department of Chemical Technology, P.O. Box 217, 7500 AE Enschede, Netherlands

<sup>b</sup> Organon Teknika B.V., P.O. Box 84, 5280 AB Boxtel, Netherlands

Received 22 November 1993; accepted in revised form 16 September 1994

### Abstract

Inverse size exclusion chromatography (i-SEC) was used to characterize three different cellulosic hollow fiber hemodialysis membranes, i.e. low-flux cuprophane and hemophane and high-flux RC-HP400A. With the i-SEC technique the pore size distribution and porosity of a membrane can be determined and adsorption phenomena can be studied. The membranes showed clear differences in pore size and porosity, the high-flux RC-HP400A membrane has a larger pore size as well as a higher porosity. For all the membranes it was found that the elution curves were best described by a homoporous pore volume distribution. It appeared that the bound or non-freezing water in the membranes was at least partly accessible to solutes. The test molecules creatinine and vitamin B12 both adsorbed to the cellulosic membranes. The adsorption behavior of creatinine was strongly dependent on the NaCl concentration present. The observations could be explained by assuming that cuprophane and RC-HP400A are negatively charged whereas hemophane is positively charged due to the modification with *N,N*-diethylaminoethyl ether. The net charge of the hemophane is smaller.

**Keywords:** Artificial kidney; Dialysis; Membrane preparation and structure; Membrane characterization; Chromatography

### 1. Introduction

Size exclusion chromatography (SEC) is a widely employed technique for the separation of solutes according to their size. It is also applied as a standard technique for the determination of the size and molecular weight of (macro)molecules. If well-defined tracer molecules are taken instead, inverse size exclusion chromatography (i-SEC) can be used to study the morphology of porous materials.

For the characterization of cellulosic hemodialysis membranes only a limited number of characterization techniques for porous structures are useful [1]. Because the pores in these membranes develop upon swelling in water wet-state characterization techniques are essential. Besides, dialysis membranes are typically used to separate low and high molecular weight solutes in a solution, which means that the characteristic or average pore size is just a few nanometers. For low-flux cuprophane membranes pore radii of 2–3 nm are reported in the literature [2]. The characterization technique(s) to be used for a reliable evaluation of cellulosic hemodialysis membranes should be capable of determining such small pores in the wet state.

\* Corresponding author.

<sup>1</sup> Present address: Agrotechnological Research Institute (ATO-DLO), P.O. Box 17, 6700 AA Wageningen, Netherlands.

Several authors studied the structure of cellulose used in the paper and textile industry by means of i-SEC techniques. Stone and Scallan [3] developed a static method based on depletion measurements with a range of standard molecules. The method was shown to be very time consuming and susceptible to disturbances. Especially for the hollow fiber geometry it is difficult to get accurate results because it is difficult to remove water from the lumen of the fiber. Rowland et al. [4,5] performed i-SEC measurements with preparative chromatography columns packed with ball-milled decrystallized cotton. Only with these ball-milled materials homogeneous and stable columns could be obtained. The grounding procedure, however, affected the structure of the cellulose. Recently Bredereck et al. [6–8] and Grünwald et al. [9] reported on i-SEC studies with packed HPLC-columns. By packing the columns with pieces of material cut to small size, stable columns and reproducible results could be obtained. Bredereck et al. reported good correlations between their i-SEC results and, e.g. iodide sorption, BET internal surface area and dyeing characteristics [6]. Moreover, we learned from personal communications with Bredereck and Hoffman-Frey that the i-SEC technique can be well employed to study the structure of other swollen cellulosic materials such as hemodialysis membranes.

The i-SEC technique has several advantages compared to other membrane characterization techniques such as retention or diffusion measurements. i-SEC measurements are not disturbed by concentration polarization, and because the membrane material is cut into small pieces the method is not hampered by the geometry of the hollow fiber. An additional advantage is that only very small amounts of tracer are needed. Finally, i-SEC measurements allow the discrimination between adsorption and geometrical effects: by comparing the elution volume of a certain substance with a standard elution curve interaction effects can be studied. The i-SEC technique is not suitable for studying the structure of anisotropic membranes.

## 2. Theoretical

### 2.1. Principle

Size exclusion chromatography is based on the principle that dependent on its size a molecule is more-or-

less able to enter the pores of a porous material. When a column is packed with a porous material and an eluent is forced through, injected molecules that are too large to enter the pores will be eluted in the so-called 'void volume' of the column. Very small tracer molecules are able to penetrate into (almost) all the pores of the material and the measured elution volume corresponds accordingly with the sum of the total pore volume and the void volume of the column. The measured elution volume of a tracer is a function of the distribution coefficient of the tracer in the material:

$$V_e = V_0 + K \cdot V_p^t \quad (1)$$

where  $V_e$  is the elution volume of the tracer,  $V_0$  the void volume of the column,  $K$  the distribution coefficient of the tracer and  $V_p^t$  the total volume of the pores in the column.

The distribution coefficient of non-adsorbing molecules is only determined by the size and shape of the tracer and the size distribution and the shape of the pores. For a reliable characterization of a porous structure the following basic experimental conditions should be satisfied:

- no adsorption interaction between tracer molecules and porous material
- the elution rate should be sufficiently slow to allow equilibrium distribution of the tracers in the pores
- low tracer concentrations to avoid intermolecular interactions between tracer molecules in the eluent
- the tracer molecules should be well defined (shape, size, preferably no size distribution) and should not deform due to the pressure drop over the column

For the characterization of water swollen cellulosic materials lower alcohols, mono- and oligo-saccharides, dextrans and polyethylene glycols are reported to be suitable tracers [7,8].

### 2.2. Equilibrium partitioning of molecules in pores

The i-SEC technique uses a wide range of tracer molecules with largely different dimensions. The smallest tracer molecules can be considered as rigid spheres. The large macromolecules do behave as flexible random-coil polymer chains. Essentially two classes of solute partitioning models have been proposed, i.e. for rigid and for flexible molecules.

The partitioning of rigid spherical solutes in pores of different shapes is given by an equation of Giddings [10]:

$$K = (1 - q)^\alpha \quad q \leq 1 \quad (2)$$

$$K = 0 \quad q > 1$$

where  $K$  is the distribution coefficient of the tracer,  $q$  is the ratio of the solute radius  $r$  and the pore radius  $R_p$  and  $\alpha$  is the pore shape factor. For slit-shaped pores  $\alpha = 1$ , for cylindrical pores  $\alpha = 2$  and for spherical pores  $\alpha = 3$ .

The partitioning of random-coil macromolecules in pores of various shapes was analyzed by Casassa et al. [11–13]. The result is a relation for the distribution coefficient of a macromolecule with a radius of gyration  $r_g$  in a pore with radius  $R_p$ :

$$K^{(\alpha)} = \sum_{m=1}^{\infty} \frac{2\alpha}{[\beta_m^{(\alpha)}]^2} \cdot \exp\left[-\left(\beta_m^{(\alpha)} \cdot \frac{r_g}{R_p}\right)^2\right] \quad (3)$$

For slit-shaped pores  $\alpha = 1$  and  $\beta_m^{(\alpha=1)} = \pi(m - 0.5)$ , for cylindrical pores  $\alpha = 2$  and  $\beta_m^{(\alpha=2)}$  is the  $m^{\text{th}}$  root of the Bessel function  $J_0(\beta)$ , for spherical pores  $\alpha = 3$  and  $\beta_m^{(\alpha=3)} = \pi m$ . In wide pores, i.e.  $R_p \gg r_g$ :

$$K^{(\alpha)} \approx 1 - \frac{2\alpha}{\sqrt{\pi}} \cdot \frac{r_g}{R_p} \quad (4)$$

Eq. 4 indicates that for wide pores the initial course of the SEC curve is linear. An important result of Casassa's work is that with large macromolecules and narrow pores at  $r_g > R_p$ , the distribution coefficient is not equal to zero. This means that a number of larger macromolecules penetrate into narrow pores, assuming elongated conformations that are different from the equilibrium conformation of the macromolecules in solution.

Eq. 4 acquires the most universal and model-independent form for the distribution coefficient in wide pores if a transition is made from the radius of gyration of the macromolecule to its effective chromatographic radius  $s = 2r_g/\sqrt{\pi}$ . Gorbunov et al. [14] introduced the parameter  $\Sigma = \alpha/R_p = S_p/V_p$ , the ratio of pore surface  $S_p$  to pore volume  $V_p$  instead of the pore radius  $R_p$ :

$$K^{(\alpha)} \approx 1 - s\Sigma \quad (5)$$

The  $K^{(\alpha)}$  versus  $s\Sigma$  relationships for different pore shapes are shown in Fig. 1. The curves show a linear dependence of  $K$  for small values of  $s\Sigma$ . Plotted in these coordinates, the three different curves are rather close

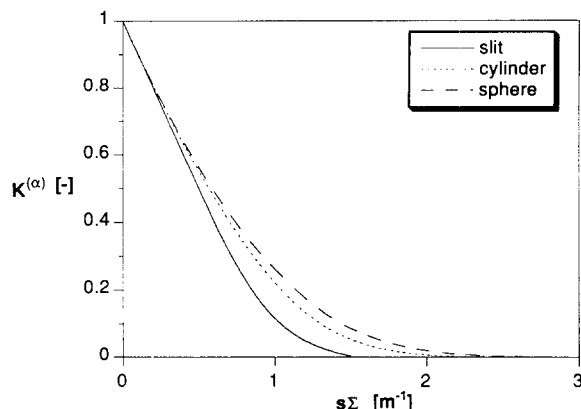


Fig. 1. The  $K^{(\alpha)}$  versus  $s\Sigma$  relationships for the different pore geometries.

to one another and at  $s\Sigma < 0.4$  they almost coincide. Consequently, i-SEC measurements cannot be used to obtain reliable information about the pore form of the sorbent.

### 2.3. Determination of pore volume distributions from SEC curves

In an excellent paper Gorbunov et al. [14] reviewed different methods of calculating pore volume distributions from SEC curves. The relative pore volume distribution function  $f_v(R_p)$  is defined by:

$$f_v(R_p) = \frac{1}{V_p} \cdot \frac{dV}{dR_p} \quad (6)$$

where  $V$  is the volume of pores with a radius between  $R_p$  and  $R_p + dR_p$  and  $V_p$  is the total pore volume of the membrane.

Gorbunov [15] introduced differential functions for the pore volume distribution  $f_v(R_p)$  and for the pore surface distribution  $f_s(R_p)$ , normalized for the total pore volume  $V_p$  and for the total pore surface area  $S_p$ . The mean radii  $R_v$  and  $R_s$  corresponding to these functions are defined by the following relationships:

$$R_v = V_p^{-1} \int_0^{\infty} R f_v dR = R_s^{-1} \cdot S_p^{-1} \int_0^{\infty} R^2 f_s(R) dR \quad (7)$$

$$R_s = S_p^{-1} \int_0^{\infty} R f_s dR = V_p \left[ \int_0^{\infty} R^{-1} f_v(R) dR \right]^{-1} = \alpha \frac{V_p}{S_p} \quad (8)$$

Also for polydisperse sorbents the initial course of the  $\bar{K}(r)$  relationship is described by a simple universal equation:

$$\bar{K}(r) \approx 1 - \frac{2\alpha}{\sqrt{\pi}} \cdot \frac{r}{R_s} = 1 - s\Sigma \quad r \ll R_s \quad (9)$$

where  $\bar{K}(r)$  is the mean distribution coefficient for a polydisperse sorbent. The initial slope of the  $\bar{K}(r)$  relationship depends only on the specific surface area of the sorbent  $\Sigma$  (or mean pore radius  $R_s$ ), and is independent of the width and type of the pore size distribution function.

When the sizes of the tracer molecules are comparable to the pore radius  $R_s$  the distribution coefficient becomes dependent on the width and type of the function  $f_v(R_p)$ . Gorbunov et al. [14] calculated SEC curves for different pore size distribution functions. The final result of their calculations was that the SEC curves depend mainly on two parameters, the mean pore radius  $R_s$  and the width of the pore size distribution function  $U$ . The type of distribution function has only little effect.

For a polydisperse sorbent the distribution coefficient function  $\bar{K}(r)$  is calculated as:

$$\bar{K}(r) = \frac{1}{V_p} \int_0^{\infty} K(r/R_p) \cdot f_v(R_p) dR_p \quad (10)$$

Eq. 10 is a so-called first-kind Fredholm equation and the problem of using this equation to find an unknown function  $f_v(R_p)$  is classed among the 'ill-posed' mathematical problems. This implies that for all practical purposes minor errors in the initial data will have a considerable effect on the calculated results. The same problem is encountered for the determination of pore volume distributions from sieving coefficients or retention data [16,17]. Mason et al. [16] and Leypoldt [18] concluded that there is not a single solution to the problem unless some assumption is made about the shape of the pore volume distribution.

Gorbunov proposed a procedure which consists of approximating the experimental  $K^{(1)}(r_i)$  relationship obtained by using a series of tracer molecules of known radii  $r_i$ , by means of the theoretical Eq. 10. The kernel of the procedure is the  $K(r/R_p)$  function of the form of Eq. 3, whereas the desired distribution  $f_v(R_p)$  is specified by a 'logarithmic normal law' (Eq. 12) with

varying parameters  $R_s$  and  $U$ . A set of parameters ( $R_s$ ,  $U$ ,  $V_p$ ) is searched to find those which minimize the function:

$$T(R_s, U, V_p) = \sum_i (K_i^{\text{exp}} - K_i)^2 \quad (11)$$

where  $R_s$  is the mean pore size (Eq. 8),  $U$  the pore volume distribution width, the experimentally observed distribution coefficient and  $K_i$  the calculated distributed coefficient. The logarithmic normal distribution function is given by:

$$f_v(R_p) = \frac{V_p}{R_p \sqrt{2\pi \ln(U)}} \cdot \exp \left[ - \frac{\left( \ln \left( \frac{R_p}{R_s \sqrt{U}} \right) \right)^2}{2 \ln(U)} \right] \quad (12)$$

### 3. Experimental

#### 3.1. Tracers

A critical point in the i-SEC analysis is the size assessment of the tracer molecules. Various methods are described in the literature to determine the dimensions of the tracer molecules. Characteristic sizes were derived for instance from diffusion and sedimentation coefficients and from viscosity and turbidity measurements. The different methods all give a characteristic dimension but it is rather uncertain which parameter gives the best results with size exclusion chromatography. This is also important because tracer molecules often have a molecular size distribution. Furthermore, changes in the actual size of the tracer can (easily) arise because of the flow-induced deformation of the flexible tracer molecules. Several authors reported on this phenomenon [19–21]. Squire [22] mentioned that especially polyethylene glycols are susceptible to deformation.

For the size determination of dextrans Bredereck [23] used an equation of Haller [24] based on viscosimetric data:

$$r = 0.027M^{0.5} \quad [nm] \quad (13)$$

where  $r$  is the tracer radius and  $M$  is the molecular weight of the tracer.

Table 1  
Characteristics of the tracers used

Tracer	$M$ [g mol <sup>-1</sup> ]	$r$ [nm]
Creatinine	113	0.28
Vitamin B12	1355	0.78
D <sub>2</sub> O	20	0.11
Methanol	32	0.23
D-Glucose	180	0.36
Maltose	342	0.49
Maltotriose	504	0.58
Maltotetraose	667	0.66
Maltopentaose	824	0.72
Maltohexaose	991	0.79
Maltoheptaose	1153	0.84
PEG 200	200	0.73
PEG 400	400	0.96
PEG 600	600	1.12
PEG 1000	1 000	1.41
PEG 1500	1 500	1.63
PEG 2000	2 000	1.82
PEG 3000	3 000	2.20
PEG 4000	4 000	2.40
PEG 6000	6 000	2.83
Dextran T10	10 000	2.68
Dextran T40	40 000	4.86
Dextran T70	70 000	6.35
Dextran T500	500 000	14.5
Dextran T2000	2 000 000	37.5

For the polyethylene glycols a relation of Squire [22] based on SEC data was used:

$$r = 0.087M^{0.4} \quad [nm] \quad (14)$$

For sugars and oligosaccharides Bredereck used data of Brown and Johnsen [25] based on Stokes radii. For our work we used mono- and oligo-saccharides ( $n = 1$  to 7) of glucose. The radii of these molecules were calculated from an equation which was obtained by fitting the data of Bredereck to a power-law:

$$r = 0.037M^{0.47} \quad [nm] \quad (15)$$

The radii of methanol and D<sub>2</sub>O were taken from Bredereck and Klein et al. [26], respectively. Data for creatinine and vitamin B12 are based on Stokes radii, the diffusion coefficients were measured using a Taylor capillary dispersion technique in a set-up described by Snijder et al. [27]. The characteristics of the tracers used for this study are listed in Table 1. The dextrans were purchased from Pharmacia, the polyethylene glycols from Fluka and all other tracers from Merck.

Tracer concentrations of 1 g dm<sup>-3</sup> (0.1%) in water were used and a volume of 50 mm<sup>3</sup> was injected. For the determination of the elution volumes of D<sub>2</sub>O and methanol 5 and 3 mm<sup>3</sup> of the pure substance were injected, respectively. To prevent growth of microorganisms 200 mg dm<sup>-3</sup> formaldehyde was added to the samples. Small quantities of the filtered tracer solutions were stored separately at -18°C.

### 3.2. HPLC system

The HPLC system consisted of a Waters 610 HPLC pump with a 600E pump controller, a 410 refractive index detector, a column oven and a 746 integrator.

### 3.3. Column material

For the studies three different types of hollow-fiber cellulosic hemodialysis membranes were used, i.e. low-flux cuprophane<sup>®</sup> and hemophan<sup>®</sup> and high-flux RC-HP400A. The low-flux fibers, with a dry wall thickness of 8 μm, were provided by Organon Teknika, Boxtel, The Netherlands. The high-flux RC-HP400A fibers were provided by Enka, Wuppertal, Germany. The cuprophane and RC-HP400A fibers are made of a regenerated cellulose. The hemophane fibers are made of a regenerated and modified cellulose. In order to improve its biocompatibility the cellulose of hemophane has been modified with a small amount of (positively charged) *N,N*-diethylaminoethyl (DEAE) ether groups.

### 3.4. Column preparation

The fibers were cut into pieces of about 0.5–1 mm using scissors. Unless stated otherwise, the fibers were swollen in water and the water was decanted several times to remove impurities as much as possible. The column (300 × 7.5 mm internal diameter, stainless steel) was filled with the swollen fibers by pressing manually with a suitable piston. After closing, the column was eluted overnight with the eluent, no additional treatments were applied to avoid channeling. The eluent was degassed and filtered over a 0.2 μm filter before use. To prevent the growth of microorganisms 200 mg dm<sup>-3</sup> formaldehyde was added to the eluent. In general, a stable detector signal was obtained after running overnight with eluent. The void volume of each column was determined from the elution volume of

dextran T2000 ( $M = 2\,000\,000\text{ g mol}^{-1}$ ). The elution volumes were determined from the peak maxima.

After the runs, the columns were dried in a vacuum oven at  $80^\circ\text{C}$  till a constant weight was reached and the weight of the column material was determined.

### 3.5. Water content of the fibers

The equilibrium water content of the swollen fibers was determined with a centrifuge method based on DIN-53814 [28]. In a small centrifuge tube, a tube provided with a microfiltration membrane in the bottom was mounted (Millipore Ultrafree-MC); this tube was filled with swollen fiber pieces of about 1.5 cm. The material was centrifuged for 20 min at 900g to remove excess water. The water content of the samples was determined from the weight decrease upon drying the centrifuged fibers overnight in a vacuum oven at  $80^\circ\text{C}$ .

### 3.6. Pore size modelling

The pore size distributions were determined by minimizing Eq. 11 using the Eqs. 10 and 12. A cylindrical pore geometry was assumed. Since for the measurements both small rigid and large flexible tracers were used the partitioning models were arbitrarily chosen as follows:

$r < R_p$ : rigid exclusion model of Giddings (Eq. 2)

$r \geq R_p$ : flexible exclusion model of Casassa (Eq. 3)

The fitting procedure was implemented in the spreadsheet program Excel using a minimization routine of Newton. The accessible pore volumes of all tracers with water as the eluent, except vitamin B12 and creatinine, were used in the fitting procedure.

## 4. Results and discussion

### 4.1. Packing of the column

The packing of the column is an important parameter. When the column is packed too loose channeling, i.e. irregular flow of the eluent occurs. On the other hand, when the packing is too tight this will result in

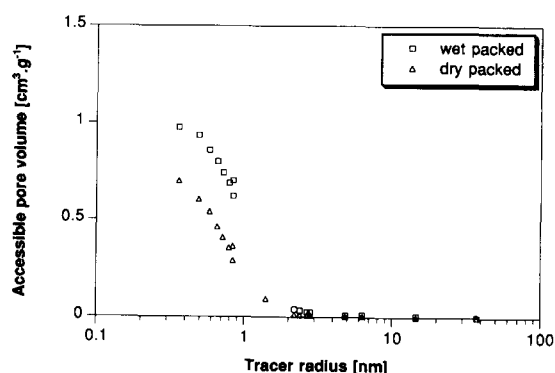


Fig. 2. Elution curves of differently packed cuprophan columns.

incomplete swelling of the column material and hence in a membrane structure which deviates from the structure under normal dialysis conditions. Fig. 2 shows two elution curves of columns packed with cuprophan fibers. The first curve is of a column packed with swollen cuprophan as described in the experimental section. The second curve is of a column which is packed with dry cuprophan and then eluted to allow swelling of the fiber material. It is obvious that the latter procedure does not allow the membrane to swell completely. For one of the columns tested it was not even possible to obtain any flow of eluent through the column.

For the low-flux fibers reproducible results could be obtained by packing the column with wet fiber material. Since the columns were never filled with exactly the same amount of fiber material this is an indication that no channeling occurred. For the high-flux fiber, however, special care had to be taken to obtain columns with a completely swollen matrix. Only by packing the swollen fibers very carefully and without pressing also for the high-flux fibers reproducible results could be obtained. Fig. 3 shows the effect of column packing on the calculated membrane parameters.

### 4.2. Choice of the experimental conditions

The elution rate in an i-SEC column should be sufficiently low to obtain equilibrium partitioning of the tracers between the pores and eluent. Fig. 4 shows the effect of the elution rate on the elution volume of several tracers. In particular the elution volumes of maltose and maltoheptaose are dependent on the flow rate. The dashed parts of the curves indicate the estimated elution volumes extrapolated to elution rate zero. The curves

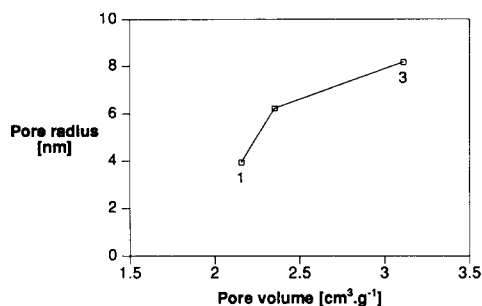


Fig. 3. Relation between pore radius and pore volume of three different columns filled with high-flux RC-HP400A; the packing density of the columns was varied, 1: high packing density, 3: low packing density.

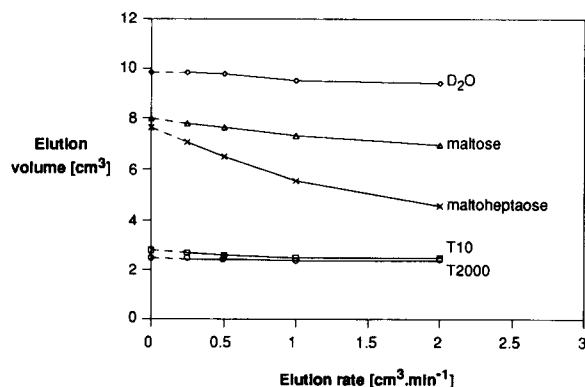


Fig. 4. Relation between the elution volume and the elution rate for several tracers,  $T=37^{\circ}\text{C}$ , cuprophane.

were extrapolated by fitting second order polynomials to the measured data.

Since the time needed to obtain equilibrium partitioning is expected to decrease with increasing temperature the elution volumes of the tracers were also determined at elevated temperatures. In Table 2 the elution volumes are listed as a percentage of the estimated elution volume at elution rate zero and for various temperatures. For all the tracers shown a flow rate of  $0.25\text{ cm}^3\text{ min}^{-1}$  and a column temperature of  $50^{\circ}\text{C}$  are sufficient to approach equilibrium conditions reasonably well ( $\geq 95\%$ ). For the following measurements a flow rate of  $0.25\text{ cm}^3\text{ min}^{-1}$  and a temperature of  $70^{\circ}\text{C}$  were chosen. The temperature of  $70^{\circ}\text{C}$  is probably not too high for the column material; as shown in Table 2 only small differences between  $50$  and  $70^{\circ}\text{C}$

are found. Grünwald et al. [9] reported that no changes of the column material occurred at temperatures up to  $90^{\circ}\text{C}$ .

Bredereck et al. [23] and Grünwald et al. [9] reported that linear flow velocities of maximal  $4.4\text{ cm min}^{-1}$  at  $20^{\circ}\text{C}$  gave acceptable results for most column materials and tracers. The columns used in this study all have a void volume of at least  $2.5\text{--}3\text{ cm}^3$ . A linear flow velocity of  $4.4\text{ cm min}^{-1}$  thus corresponds to an elution rate of about  $0.4\text{ cm}^3\text{ min}^{-1}$ . The flow rates used in this study ( $0.25\text{ cm}^3\text{ min}^{-1}$ ) are therefore sufficiently small.

#### 4.3. Elution curves

The elution curves of the different membrane materials are shown in Figs. 5–7. The most remarkable result is the difference in total accessible pore volume between the high- and low-flux fibers. The set of chosen tracer molecules covers the complete range of relevant tracer radii. Most of the tracers shown do fit a smooth S-shaped curve, as was expected. It appears therefore that the tracer dimensions were estimated adequately and that no deformation of the tracers occurred. Some

Table 2

Estimated elution volumes as a percentage of the extrapolated values for elution rate zero at different elution rates and column temperatures

Tracer	Rate [ $\text{cm}^3\text{ min}^{-1}$ ]	0.25	0.5	1.0	2
	$T$ [ $^{\circ}\text{C}$ ]				
T2000	37	98	97	95	96
	50	100	100	100	100
	70	100	100	100	100
T10	37	97	93	90	89
	50	99	97	95	93
	70	100	100	98	96
PEG600	37				
	50	97	95	91	89
	70	99	98	94	90
Maltoheptaose	37	92	84	73	60
	50	96	93	87	78
	70	97	96	91	87
Maltose	37	97	96	91	87
	50	98	95	92	90
	70	97	93	90	82
D20	37	100	100	97	96
	50	100	100	98	98
	70	99	99	98	97

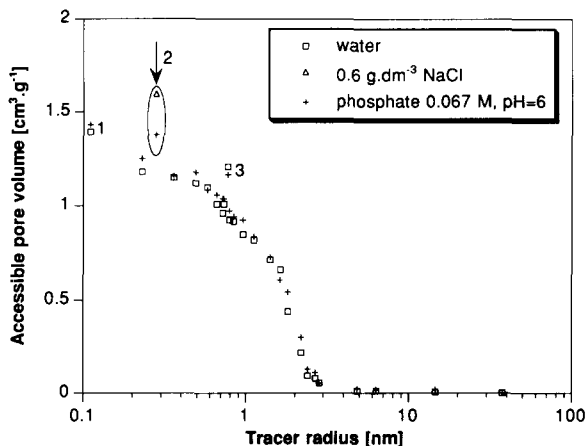


Fig. 5. Elution curves of cuprophon,  $T=70^{\circ}\text{C}$ , elution rate  $0.25\text{ cm}^3\text{ min}^{-1}$  (1:  $\text{D}_2\text{O}$ , 2: creatinine, 3: vitamin B12).

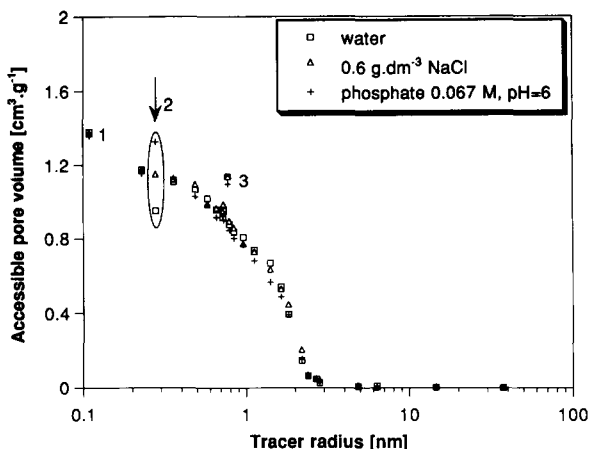


Fig. 6. Elution curves of hemophan,  $T=70^{\circ}\text{C}$ , elution rate  $0.25\text{ cm}^3\text{ min}^{-1}$  (1:  $\text{D}_2\text{O}$ , 2: creatinine, 3: vitamin B12).

tracers, however, deviate from the curve indicating that adsorption effects may be present.

The tracer indicated with number 1 in the figures represents  $\text{D}_2\text{O}$ . This molecule seems to have a somewhat larger elution volume than expected. The same phenomenon was also reported by Bredereck et al. [23] and other authors [29] for different kinds of cellulosic materials. They suggested that an adsorption effect, probably owing to  $-\text{OD}/-\text{OH}$  exchange is present. Bredereck et al. found a slight decrease of the elution volume of  $\text{D}_2\text{O}$  when the temperature of the column was increased (3% when the temperature was increased from  $20$  to  $80^{\circ}\text{C}$ ). An increased temperature is expected

to reduce the extent of adsorption. The decrease of 3%, however, was insufficient to explain the deviating elution volume of  $\text{D}_2\text{O}$ . Bredereck also found that the difference in elution volume of  $\text{D}_2\text{O}$  and methanol (no adsorption) was strongly fluctuating for different kinds of samples. They suggested that a small part of the total pore volume is excluded from tracer penetration and accessible only to water or  $\text{D}_2\text{O}$ . Only the very small and polar water or  $\text{D}_2\text{O}$  molecule is able to penetrate into the narrowest pores between some cellulose chains (disordered crystallite surfaces). When water was replaced by methanol as eluent, both deuterated methanol ( $\text{MeOD}$ ) and  $\text{D}_2\text{O}$  approximately had the same elution volume. Apparently the change in eluent resulted in a disappearance of the very small pores that exist in water swollen cellulose. Although Bredereck did not use the term bound water it might be that these pores are filled with so-called bound or non-freezing water and therefore they are not accessible to other molecules than water. Bredereck reported a good agreement between the accessible pore volume of  $\text{D}_2\text{O}$  and the water content of the membrane as determined with the centrifuge method according to DIN-53814.

The test molecules creatinine and vitamin B12 both appear to adsorb to the cellulosic membranes, the apparent accessible pore volumes are higher than expected on the basis of their size. For the cuprophon and RC-HP400A fibers no elution peak of creatinine can be observed using pure water as eluent. With an eluent containing  $0.6\text{ g dm}^{-3}\text{ NaCl}$  the accessible pore

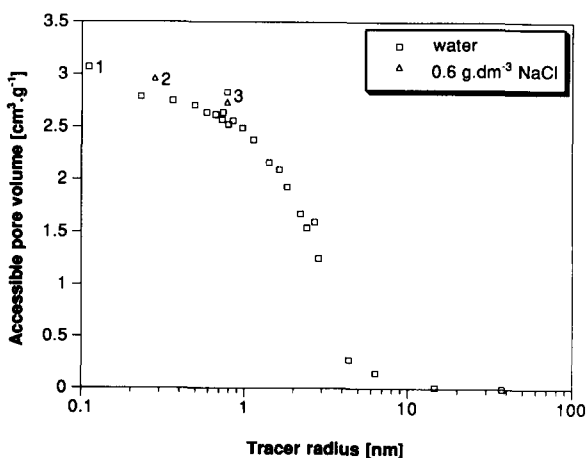


Fig. 7. Elution curve of RC-HP400A,  $T=70^{\circ}\text{C}$ , elution rate  $0.25\text{ cm}^3\text{ min}^{-1}$  (1:  $\text{D}_2\text{O}$ , 2: creatinine, 3: vitamin B12).

volume is somewhat higher than expected. Fig. 8 shows the effect of the NaCl concentration on the elution volume of creatinine and dextran T2000 on a cuprophane column. The elution volume of creatinine is a strong function of the NaCl concentration in the eluent. For very low concentrations creatinine is strongly adsorbed to the cuprophane matrix. Colton et al. [30] determined the distribution coefficient of creatinine for a cuprophane flat sheet membrane by depletion measurements. They reported no adsorption of the creatinine, their results, however, were obtained from depletion measurements in an isotonic NaCl solution ( $9 \text{ g dm}^{-3} \text{ NaCl}$ ).

The adsorption behavior of creatinine on hemophan is opposite. Using water as the eluent the apparent accessible pore volume of creatinine is somewhat smaller than expected, the creatinine is partly excluded. For eluentia with a higher ionic strength the accessible pore volume for creatinine increases. For high NaCl concentration the accessible pore volume is higher than expected indicating that additionally an other adsorption mechanism may be present. The adsorption effects are much less dependent on the NaCl concentration.

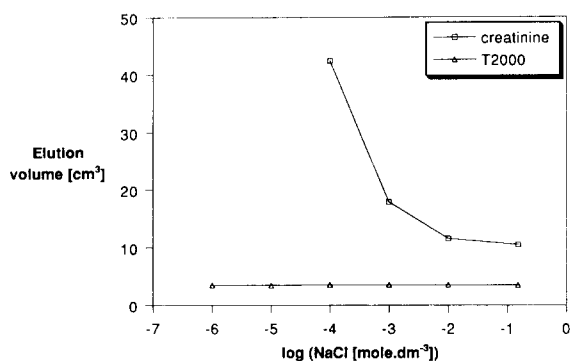


Fig. 8. Elution volumes of creatinine and T2000 as a function of the NaCl concentration for a cuprophane column.

Table 3

Calculated and measured membrane parameters, assuming a cylindrical pore shape

Membrane	H <sub>2</sub> O [cm <sup>3</sup> g <sup>-1</sup> ]	V <sub>p</sub> [cm <sup>3</sup> g <sup>-1</sup> ]	V <sub>D<sub>2</sub>O</sub> measured [cm <sup>3</sup> g <sup>-1</sup> ]	V <sub>D<sub>2</sub>O</sub> calcd [cm <sup>3</sup> g <sup>-1</sup> ]	R <sub>p</sub> [nm]	U [-]
Cuprophane	1.48	1.48	1.41	1.40	4.1	1
Hemophane	1.57	1.45	1.38	1.36	3.7	1
RC-HP400A	3.08	3.11	3.07	3.03	8.2	1

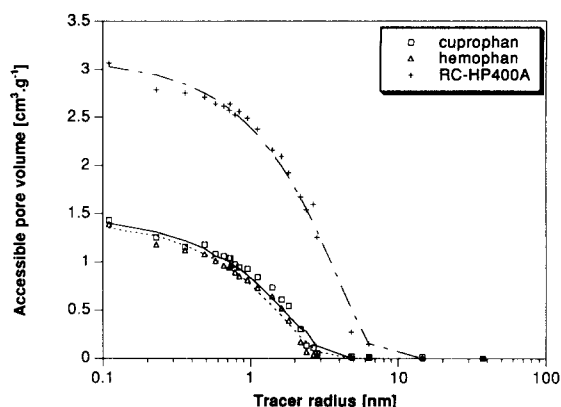


Fig. 9. Measured and calculated elution curves. The lines represent the calculated curves based on the parameters  $V_p$  and  $R_p$  of Table 3.

These results indicate that an electrostatic interaction is responsible for the adsorption behavior of creatinine. The creatinine molecule is a weak base and can adopt a positive charge [31]. Regenerated celluloses contain a small amount of carboxylic groups which cause a negative charge [32]. The hemophane fibers have been modified with positively charged DEAE groups. From the curves in Fig. 6 it appears that the hemophane has a net positive charge although the net amount of charge is smaller than for the cuprophane and RC-HP400A fibers.

The accessible pore volume for vitamin B12 is hardly influenced by the ionic strength of the eluent indicating that no electrostatic interaction is responsible for its adsorption behavior.

#### 4.4. Pore size determination

The calculated and measured membrane parameters are shown in Table 3. For all the membranes it is found that the elution curves are best described by a homoporous pore size distribution, i.e.  $U=1$ . In Fig. 9 the

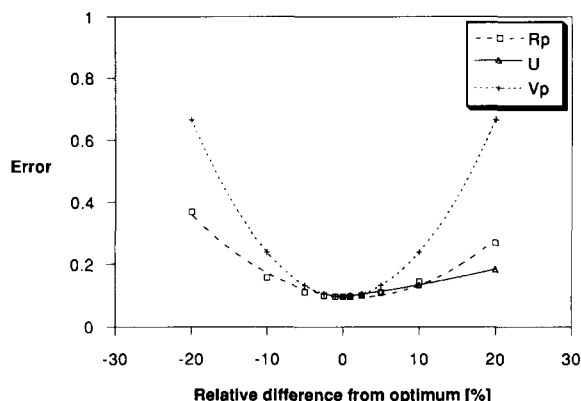


Fig. 10. Sensitivity of the model to its parameters. Data were calculated for a cuprophane column.

measured and calculated elution curves of the different membranes are shown. The lines represent the calculated curves based on the membrane parameters,  $V_p$ ,  $U$  and  $R_p$ , shown in Table 3. All curves are well described with a homoporous pore volume distribution. In the fitting procedure the sum of the absolute differences between experimental and calculated distribution coefficients is minimized. This means that mainly the small solutes contribute to the sum of errors. The distribution coefficient of small solutes is relatively insensitive towards a distribution of pores. Still, also fitting of the curves by minimizing the sum of relative errors resulted in a homoporous pore volume distribution function.

Fig. 10 shows the sensitivity of the model towards its parameters. The model is most sensitive to the pore volume parameter. It is rather insensitive to the distribution width and this may also explain why homoporous pore volume distributions are found. Although actually no pore size (volume) distributions of regenerated cellulose membranes are reported in the literature also other authors got indications that the pore size distributions in these membranes must be very narrow indeed [2,33].

In Table 3 four different estimates for the total pore volume of the membranes are given. The first column ( $H_2O$ ) gives the equilibrium water content as measured with the centrifuge method described in the experimental part. The second column ( $V_p$ ) contains the optimal fit for the pore volume. The third ( $V_{D_2O}$  measured) and fourth column ( $V_{D_2O}$  calcd) represent the measured and calculated accessible pore volume for  $D_2O$ , respectively. Since the  $D_2O$  molecule has a finite dimension

this value is somewhat smaller than the fitted pore volume  $V_p$ .

The listed estimates for the total pore volume coincide very well indicating that the membranes were completely swollen. Only for the hemophan columns the obtained value for  $V_p$  appears to be somewhat too low. The measured data for the accessible pore volume for  $D_2O$  are about 5% smaller than the  $H_2O$  content. This may be explained by the different temperatures used for the determination of the water content and the i-SEC measurements.

The accessible pore volume of the high-flux fiber is more than twice the pore volume of the low-flux fibers. Also the pore radius of the high-flux fiber appears to be about twice as large. For low-flux cuprophane membranes cylindrical pore radii of 2–3 nm are reported in the literature [2]. The radius of 4.1 nm given in Table 3 is (somewhat) larger.

From the curves in Fig. 9 it appears that some of the smaller tracers do not fit the calculated curves. For all three curves methanol and glucose have a measured accessible pore volume which is smaller than the calculated values. The  $D_2O$  data points do fit the calculated curves. The observations may be explained partly by assuming, as Bredereck et al. did, that some of the pores in the membranes are so small that they can only contain a water or  $D_2O$  molecule. It might be that these water molecules form the non-freezing or bound water of the membrane. The non-freezing water content of these membranes was determined as  $0.48 \text{ g g}^{-1}$  for the low-flux membranes and  $0.73 \text{ g g}^{-1}$  for the high-flux membrane [34]. These values were determined with a calorimetric method at temperatures below  $0^\circ\text{C}$ . The i-SEC measurements are performed at a (much) higher temperature. It may be that for these higher temperatures the amount of bound water is different. Bound or non-freezing water is often assumed to be not accessible to solutes. The differences between the accessible pore volume for  $D_2O$  and methanol are only about 0.2 and  $0.28 \text{ g g}^{-1}$  for the low- and high-flux membrane, respectively. These values are much smaller than the values determined with the calorimetric method suggesting that at least some of the non-freezing water may be accessible for other molecules. If a part of the water in the membranes is present as not accessible bound water then it may be expected that the fitted parameter  $V_p$  is smaller than the measured pore volume from the

water content. From Table 3 it appears that this is not the case, both parameters coincide very well.

## 5. Conclusions

The i-SEC technique is an elegant and, for the purpose of membrane characterization, very useful technique. The pore size distributions of symmetrical or isotropic membranes can be determined and adsorption phenomena can be studied.

The membranes used in this study show clear differences in pore size and porosity. The high-flux RC-HP400A membrane has a larger pore size as well as a larger porosity than the two low-flux membranes. For all the membranes it is found that the elution curves are best described by a homoporous pore volume distribution. It appears that at least some of the bound or non-freezing water in the membranes is accessible to the tracer molecules.

The adsorption behavior of the test molecule creatinine is influenced by the NaCl concentration of the eluent, indicating that an electrostatic interaction is present. The observations can be explained by assuming that the cuprophan and RC-HP400A fibers are negatively charged and the hemophan fiber is positively charged due to its modification with DEAE. The net charge of the hemophan fiber, however, is smaller.

## 6. List of Symbols

$f_v$	differential pore volume distribution function [m <sup>3</sup> kg <sup>-1</sup> m <sup>-1</sup> ]
$H$	equilibrium water content of the swollen fiber [cm <sup>3</sup> g <sup>-1</sup> ]
$K$	distribution coefficient of the tracer [-]
$\bar{K}$	mean distribution coefficient for a polydisperse sorbent [-]
$M$	molecular weight tracer [g mol <sup>-1</sup> ]
$q$	ratio of tracer radius and pore radius [-]
$q_g$	ratio of gyration radius of the tracer and the pore radius [-]
$r$	tracer radius [m]
$r_g$	gyration radius [m]
$R_p$	pore radius [m]
$R_v$	the volume mean pore radius defined by Eq. 7 [m]

$R_s$	the surface mean pore radius defined by Eq. 8 [m]
$s$	effective chromatographic radius [m]
$S_p$	specific pore surface area of the membrane [m <sup>2</sup> kg <sup>-1</sup> ]
$T$	minimization function defined by Eq. 11
$U$	pore volume distribution width [-]
$V_e$	elution volume of the tracer [m <sup>3</sup> ]
$V_0$	void volume of the column [m <sup>3</sup> ]
$V_p$	pore volume of the membrane [m <sup>3</sup> kg <sup>-1</sup> ]
$v_p^t$	total volume of the pores in the column [-]
$\alpha$	pore shape factor [-]
$\beta_m$	parameter defined by Eq. 3 [-]
$\Sigma$	ratio of pore volume and pore surface area [m <sup>-1</sup> ]

## References

- [1] A.P. Broek, Characterization of hemodialysis membranes: membrane structure and function, Ph.D. Thesis, University of Twente, 1993, Chapter 2.
- [2] R.P. Wendt, E. Klein, E.H. Bressler, F.F. Holland, R.M. Serino and H. Villa, Sieving properties of hemodialysis membranes, *J. Membrane Sci.*, 5 (1979) 23–49.
- [3] J.E. Stone and A.M. Scallan, Structural model for the cell wall of water swollen pulp fibers, *Cell. Chem. Technol.*, 2 (1968) 343–358.
- [4] S.P. Rowland and N.R. Bertoniere, Chemical methods of studying supramolecular structure, in T.P. Nevell and S.H. Zeronian (Eds.), *Cellulose Chemistry and its Application*, Ellis Horwood, 1985, Chichester, pp. 112–137.
- [5] L.F. Martin and S.P. Rowland, Gel permeation properties of decrystallized cotton cellulose, *J. Chromatogr.*, 28 (1967) 139–142.
- [6] K. Brederbeck and A. Blüher, Die Ammoniak-Vorbehandlung und ihre Auswirkung auf die Veredlung, *Melliand Textilber.*, 72 (1991) 446–454.
- [7] K. Brederbeck and A. Blüher, A. Hoffmann-Frey, Die Bestimmung der Porenstruktur von Cellulosefasern durch Ausschlußmessung, *Das Papier*, 44 (1990) 648–656.
- [8] K. Brederbeck, E. Bader and U. Schmitt, Die Bestimmung der Porenstruktur wassergequollener Zellulosefasern, *Textilveredlung*, 24 (1989) 142–150.
- [9] M. Grünwald, E. Burtcher and O. Bobleter, HPLC determination of the pore distribution and chromatographic properties of cellulosic textile materials, *J. Appl. Polym. Sci.*, 39 (1990) 301–317.
- [10] J.C. Giddings, E. Kucera, C.P. Russell and M.N. Myers, Statistical theory for the equilibrium distribution of rigid molecules in inert porous networks, exclusion chromatography, *J. Chem. Phys.*, 72 (1968) 4397–4408.

- [11] E.F. Casassa, Equilibrium distribution of flexible polymer chains between a macroscopic solution phase and small voids, *J. Polym. Sci., Polym. Lett.*, 5 (1967) 773–778.
- [12] E.F. Casassa and Y. Tagami, Equilibrium model for gel permeation chromatography of flexible polymer chains, *Macromol.*, 2 (1969) 14–26.
- [13] E.F. Casassa, Comments on exclusion of polymer chains from small pores and its relation to gel permeation chromatography, *Macromol.*, 9 (1976) 182–185.
- [14] A.A. Gorbunov, L.Y. Solovyova and V.A. Pasechnik, Fundamentals of the theory and practice of polymer gel permeation chromatography as a method of chromatographic porosimetry, *J. Chromatogr.*, 448 (1988) 307–322.
- [15] A.A. Gorbunov, L.Y. Solovyova and V.A. Pasechnik, Determination of the characteristics of the porous structure of sorbents using gel permeation chromatography of polymers, *Vysokomol. Soedin. Ser. A*, 26 (1984) 967–973.
- [16] E.A. Mason, R.P. Wendt and E.H. Bressler, Similarity relations (dimensional analysis) for membrane transport, *J. Membrane Sci.*, 6 (1980) 283–298.
- [17] K.D. Knierim and E.A. Mason, Heteroporous sieving membranes: rigorous bounds on pore size distribution and sieving curves, *J. Membrane Sci.*, 42 (1989) 87–107.
- [18] J.K. Leypoldt, Determining pore size distributions of ultrafiltration membranes by solute sieving – Mathematical limitations, *J. Membrane Sci.*, 31 (1987) 289–305.
- [19] W.M. Deen, Hindered transport of large molecules in liquid-filled pores, *Am. Inst. Chem. Eng. J.*, 33 (1987) 1409–1425.
- [20] Q.T. Nguyen and J. Neel, Characterization of ultrafiltration membranes. Part IV. Influence of the deformation of macromolecular solutes on the transport through UF-membranes, *J. Membrane Sci.*, 14 (1983) 111–128.
- [21] S. Daoudi and F. Brochard, Flows of flexible polymer solutions in pores, *Macromol.*, 11 (1978) 751–758.
- [22] P.G. Squire, Calculation of hydrodynamic parameters of random coil polymers from size exclusion chromatography and comparison with parameters by conventional methods, *J. Chromatogr.*, 210 (1981) 433–442.
- [23] K. Bredereck and A. Blüher, Porenstrukturbestimmung von Cellulosefasern durch Ausschlußchromatographie. Grundlagen und Anwendungs-beispiele für Quellbehandlungen und Hochveredlung von Baumwollgewebe, *Melliand Textilber.*, 73 (1992) 652–662.
- [24] W. Haller, Critical permeation size of dextran molecules, *Macromol.*, 10 (1977) 83–86.
- [25] W. Brown and R.M. Johnsen, Transport from an aqueous phase through cellulosic gels and membranes, *J. Appl. Polym. Sci.*, 26 (1981) 4135–4148.
- [26] E. Klein, F.F. Holland and K. Eberle, Comparison of experimental and calculated permeability and rejection coefficients for hemodialysis membranes, *J. Membrane Sci.*, 5 (1979) 173–188.
- [27] E.D. Snijder, M.J.M. te Riele, G.F. Versteeg and W.P.M. van Swaay, Diffusion coefficients of several aqueous alkanolamine solutions, *J. Chem. Eng. Data*, 38 (1993) 475–480.
- [28] DIN 53814, Bestimmung des Wasserrückhaltevermögens von Fasern und Faden-abschnitten, October 1974.
- [29] S.P. Rowland, C.P. Wade and N.R. Bertoniere, Pore structure analysis of purified, sodium hydroxide-treated and liquid ammonia-treated cotton celluloses, *J. Appl. Polym. Sci.*, 29 (1984) 3349–3357.
- [30] C.K. Colton, K.A. Smith, E.W. Merrill and P.C. Farrell, Permeability studies with cellulosic membranes, *J. Biomed. Mater. Res.*, 5 (1971) 459–488.
- [31] H. Yasuda, L.D. Ikenberry and C.E. Lamaze, Permeability of solutes through hydrated polymer membranes. II Permeability of water soluble organic solutes, *Makromol. Chem.*, 125 (1969) 108–118.
- [32] H. Krässig, R.G. Steadman, K. Schliefer and W. Albrecht, Cellulose, in W. Gerhartz et al. (Eds.), *Ullmann's Encyclopedia of Industrial Chemistry*, VCH, Weinheim, 5th ed., Vol. A5, 1986, pp. 375–418.
- [33] A. Hoffmann-Frey and K. Bredereck, unpublished results.
- [34] A.P. Broek, Characterization of hemodialysis membranes: membrane structure and function, Ph.D. Thesis, University of Twente, 1993, Chapter 3.